Quantum transport with spin dephasing: A nonequlibrium Green's function approach

Ahmet Ali Yanik*
Department of Physics, Network for Computational Nanotechnology, Purdue University, West Lafayette, Indiana 47907, USA

Gerhard Klimeck
School of Electrical and Computer Engineering, Network for Computational Nanotechnology, Purdue University, West Lafayette, Indiana 47907, USA and Jet Propulsion Lab, Caltech, Pasadena, California 91109, USA

Supriyo Datta
School of Electrical and Computer Engineering Network for Computational Nanotechnology, Purdue University, West Lafayette, Indiana 47907, USA

(Received 2 June 2006; revised manuscript received 25 February 2007; published 17 July 2007)

A quantum transport model incorporating spin scattering processes is presented using the nonequilibrium Green's function formalism within the self-consistent Born approximation. This model offers a unified approach by capturing the spin-flip scattering and the quantum effects simultaneously. A numerical implementation of the model is illustrated for magnetic tunnel junction devices with embedded magnetic impurity layers. This model seems to explain three experimentally observed features regarding the dependence of the junction magnetoresistances (JMRs) on the barrier thickness, barrier height, and number of magnetic impurities. It is shown that small variations in magnetic impurity spin states and concentrations could cause large deviations in JMRs.

DOI: 10.1103/PhysRevB.76.045213 PACS number(s): 72.10.−d, 71.70.Gm, 72.25.Rb, 73.43.Qt

I. INTRODUCTION

Quantum transport in spintronic devices is currently a topic of great interest. Most of the theoretical work reported so far has been based on the Landauer approach[1] assuming coherent transport, although a few authors have included incoherent processes through averaging over a large ensemble of disordered configurations.[2–4] However, it is not straightforward to include dissipative interactions in such approaches. The nonequilibrium Green's function (NEGF) formalism provides a natural framework for describing quantum transport in the presence of incoherent and dissipative processes. Here, a numerical implementation of the NEGF formalism with spin-flip scattering is presented within the single-electron treatment. Equivalently, the Fermi sea and all many-body effects are neglected (such as Kondo effect or Rudermann-Kittel-Kasuya-Yosida interaction between localized impurities due to itinerant electrons). For magnetic tunnel junctions (MTJs) with embedded magnetic impurity layers, this model is able to capture and explain three distinctive experimental features reported in the literature[5–8] regarding the dependence of the junction magnetoresistances (JMRs) on (1) barrier thickness, (2) barrier height, and (3) the number of magnetic impurities. Although in this paper we restrict our treatment to the electron-impurity spin exchange interactions, the NEGF model presented here allows one to incorporate other spin exchange scattering processes involving nuclear hyperfine, electron-hole (Bir-Aranov-Pikus) and electron-magnon interactions. This model is quite general and can be used to analyze and design a variety of spintronic devices beyond the large cross-section multilayer devices explored in this article.

We start with a brief summary of the NEGF formalism with spin dephasing in Sec II before describing the detailed numerical implementation of the model along with the results in (Sec. III A) and in (Sec. III B) for MTJ's with magnetic impurity layers. The results are briefly discussed and summarized in Sec. IV.

II. MODEL DESCRIPTION

NEGF method. The problem is partitioned into channel and contact regions as illustrated in Fig. 1.[9] Components of the partitioned device can be classified in four categories.

(i) Channel properties are defined by the Hamiltonian matrix $[H]$ including the applied bias potential.

(ii) Contacts are included through self-energy matrices $[\Sigma_L]/[\Sigma_R]$ whose anti-Hermitian component

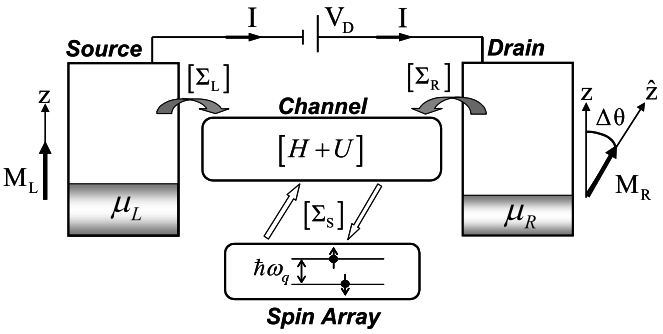

FIG. 1. A schematic illustration of device partitioning in NEGF formalism. Magnetization direction of the drain is defined relative to the source ($\Delta\theta = \theta_R - \theta_L$).

$$\Gamma_{L,R}(E) = i[\Sigma_{L,R}(E) - \Sigma_{L,R}^{\dagger}(E)], \tag{1}$$

describes the broadening due to the coupling to the contact. The corresponding inscattering/outscattering matrices are defined as

$$\Sigma_{L,R}^{\text{in}}(E) = f_0(E - \mu_{L,R})\Gamma_{L,R}(E), \tag{2a}$$

$$\Sigma_{L,R}^{\text{out}}(E) = [1 - f_0(E - \mu_{L,R})]\Gamma_{L,R}(E), \tag{2b}$$

where $f_0(E-\mu_{L,R})=1/1+\exp[(E-\mu_{L,R})/k_BT]$ is the Fermi function for the related contact.

(iii) Electron-electron interactions are incorporated through the mean field electrostatic potential matrix $[U]$.

(iv) Incoherent scattering processes in the channel region are described by in/out-scattering matrices $[\Sigma_S^{\text{in}}]/[\Sigma_S^{\text{out}}]$. Broadening due to scattering is given by

$$\Gamma_S(E) = [\Sigma_S^{\text{in}}(E) + \Sigma_S^{\text{out}}(E)], \tag{3}$$

from which the self-energy matrix is obtained through a Hilbert transform

$$\Sigma_S(E) = \overbrace{\frac{1}{2\pi}\int \frac{\Gamma_S(E')}{E' - E}dE'}^{\text{Re}} - i\overbrace{\frac{\Gamma_S(E)}{2}}^{\text{Im}}. \tag{4}$$

In a similar fashion with regular contacts [Eq. (1)], broadenings due to the scattering processes are also related with scattering self-energy matrix $[\Sigma_S]$ through

$$\Gamma_S(E) = i[\Sigma_S(E) - \Sigma_S^{\dagger}(E)]. \tag{5}$$

Equations (1)–(5) are the boundary conditions that drive the coupled NEGF equations [Eqs. (3)–(11)], where (retarded) Green's function is defined as

$$G(E) = [EI - H - U - \Sigma(E)]^{-1}, \tag{6}$$

$\Sigma(E)$ being the total self-energy due to the contacts and the scattering processes

$$\Sigma(E) = \Sigma_L(E) + \Sigma_R(E) + \Sigma_S(E). \tag{7}$$

The spectral function (whose diagonal elements are the local density of states) is defined as

$$A(E) = i[G(E) - G(E)^{\dagger}] = G^n(E) + G^p(E). \tag{8}$$

$[G^n]/[G^p]$ (commonly written as $[-iG^<]/[iG^>]$) refer the electron/hole correlation functions (whose diagonal elements are the electron/hole density)

$$G^{n,p}(E) = G(E)[\Sigma^{\text{in,out}}(E)]G(E)^{\dagger}, \tag{9}$$

where

$$\Sigma^{\text{in,out}}(E) = \Sigma_L^{\text{in,out}}(E) + \Sigma_R^{\text{in,out}}(E) + \Sigma_S^{\text{in,out}}(E). \tag{10}$$

The in/out-scattering matrices $[\Sigma_S^i]/[\Sigma_S^{\text{out}}]$ are related to the electron/hole correlation functions $[G^n]/[G^p]$ from Ref. 9 through

$$\Sigma_{S;\sigma_i\sigma_j}^{\text{in,out}}(r,r';E) = \int \sum_{\sigma_k,\sigma_l} [D_{\sigma_i\sigma_j;\sigma_k\sigma_l}^{n,p}(r,r';\hbar\omega)] \times G_{\sigma_k\sigma_l}^{n,p}(r,r';E \mp \hbar\omega)d(\hbar\omega), \tag{11}$$

where the spin indices (σ_k,σ_l) and (σ_i,σ_j) refer to the (2×2) block diagonal elements of the on-site electron/hole correlation functions and in/out-scattering matrices, respectively. Here the $[D^n]/[D^p]$ are fourth-order scattering tensors, describing the spatial correlation and the energy spectrum of the underlying microscopic spin-dephasing scattering mechanisms. In general these scattering tensors can be obtained starting from a spin scattering Hamiltonian of the form

$$H_I(\vec{r}) = \sum_{R_j} J(\vec{r} - \vec{R}_j)\vec{\sigma}\cdot\vec{S}_j, \tag{12}$$

where $\vec{r}/\vec{R}_j$ are the spatial coordinates and $\vec{\sigma}/\vec{S}_j$ are the spin operators for the channel electron/(jth) magnetic impurity. In this paper, we assume a delta interaction model (see Appendix A) and show that $[D^n]/[D^p]$ can be written as

$$D^{n,p}(r,r',\hbar\omega) = [D^{n,p}(r,r',\hbar\omega)]_{SF} + [D^{n,p}(r,r',\hbar\omega)]_{NSF}, \tag{13}$$

where the first term describing the spin-flip transitions (subscript SF) is given by

$$[D^{n,p}(r,r';\hbar\omega)]_{\text{SF}} = \delta(r-r')\sum_{\omega_q}\langle J^2\rangle N_I(\omega_q) \begin{array}{c} |\sigma_k\sigma_l\rangle\rightarrow \\ \langle\sigma_i\sigma_j|\downarrow \end{array} \begin{array}{c} \\ \langle\uparrow\uparrow| \\ \langle\downarrow\downarrow| \\ \langle\uparrow\downarrow| \\ \langle\downarrow\uparrow| \end{array} \begin{array}{c} \begin{array}{cccc} |\uparrow\uparrow\rangle & |\downarrow\downarrow\rangle & |\uparrow\downarrow\rangle & |\downarrow\uparrow\rangle \end{array} \\ \begin{bmatrix} 0 & F_{u,d}\delta(\omega \mp \omega_q) & 0 & 0 \\ F_{d,u}\delta(\omega \pm \omega_q) & 0 & 0 & 0 \\ 0 & 0 & 0 & 0 \\ 0 & 0 & 0 & 0 \end{bmatrix} \end{array}, \tag{14}$$

while the second term corresponding to the spin-conserving scatterings (subscript NSF for "no spin flip") is given by

$$[D^{n,p}(r,r';\hbar\omega)]_{\mathrm{NSF}} = \delta(r-r')\,\delta(\omega)\sum_{\omega_q}\frac{1}{4}\langle J^2\rangle N_I(\omega_q)$$

$$\begin{array}{c|c} |\sigma_k\sigma_l\rangle\rightarrow & \\ \langle\sigma_i\sigma_j|\downarrow & \end{array}$$

$$\begin{array}{c|cccc} & |\uparrow\uparrow\rangle & |\downarrow\downarrow\rangle & |\uparrow\downarrow\rangle & |\downarrow\uparrow\rangle \\ \hline \langle\uparrow\uparrow| & 1 & 0 & 0 & 0 \\ \langle\downarrow\downarrow| & 0 & 1 & 0 & 0 \\ \langle\uparrow\downarrow| & 0 & 0 & -1 & 0 \\ \langle\downarrow\uparrow| & 0 & 0 & 0 & -1 \end{array} \qquad (15)$$

Here $N_I(\omega_q)$ is the number of the magnetic impurities with $\hbar\omega_q$ energy difference between spin states and F_u/F_d represents the fractions of the spin-up/spin-down impurities for an uncorrelated ensemble $(F_u+F_d=1)$. A similar separation of SF and NSF terms was obtained by Appelbaum[10] using a tunneling-Hamiltonian treatment.

Current is calculated from the self-consistent solution of the above equations for any terminal i:

$$I_i = \int_{-\infty}^{+\infty} dE\tilde{I}_i(E), \qquad (16a)$$

$$\tilde{I}_i(E) = \left(\frac{q}{h}\right)\mathrm{tr}\{[\Sigma_i^{\mathrm{in}}(E)A(E)] - [\Gamma_i(E)G^n(E)]\}. \qquad (16b)$$

The general solution scheme without going into the details can be summarized as follows. The matrices listed under the categories (i) and (ii) are fixed at the outset of any calculations. While the $[U]$, $[\Sigma_S^{\mathrm{in,out}}]$, and $[\Sigma_S]$ matrices under the charging and scattering categories (iii) and (iv) depend on the correlation and spectral functions requiring an iterative self-consisted solution of the NEGF equations [Eqs. (3)–(11)]. One important thing to note is that for the numerical implementation presented in Sec. III we do not compute the charging potential $[U]$ self-consistently with the charge. The change in tunnel barriers is neglected and assumed not to influence the electrostatic potential. This allows one to focus on the dephasing due to the spin-flip interactions.

III. APPLICATION: MTJ'S WITH MAGNETIC IMPURITIES

In the presence of "rigid" scatterers such as impurities and defects, electron transport is considered coherent as the phase relationships between different paths are time independent and the scattering effects are incorporated into the transport problem through the device Hamiltonian H. However, the situation is different when the impurities have an internal degree of freedom, such as the internal spin states of magnetic impurities. The effect of such scatterers cannot be simply incorporated through the device Hamiltonian and scattering self-energy matrices are needed. An implementation of this self-energy matrix treatment will be discussed in this part of the paper for electron-impurity exchange scattering processes in MTJs. But first, we will discuss MTJ fundamentals and device characteristics in the absence of magnetic impurities (the coherent regime).

A. MTJs: Coherent regime

MTJs devices considered here consist of a tunneling barrier (AlO_x) sandwiched between two ferromagnets (Co) with different magnetic coercivities enabling independent manipulation of contact magnetization directions (Fig. 2). Single band tight-binding approximation is adopted[11] with an effective electron mass $(m^*=m_e)$ in the tunneling region and the ferromagnetic contacts. Accordingly for constant effective mass throughout the device, parallel $\vec{k}_{\parallel}$ components can be included using two-dimensional (2D) integrated Fermi functions in Eq. (2a):

$$f_{2\mathrm{D}}(E_z-\mu_{L,R}) = N_s\ln[1+\exp(\mu_{L,R}-E_z k_B T)], \qquad (17)$$

where $N_s=(m^*k_BT)/2\pi\hbar^2$ is defined for per unit area leading to 2D integrated in-scattering function

$${}^{2\mathrm{D}}\Sigma_{L,R}^{\mathrm{in}}(E_z) = f_{2\mathrm{D}}(E_z-\mu_{L,R})\Gamma_{L,R}(E_z). \qquad (18)$$

The Green's function of the device is simply defined as

$$G(E_z) = [E_z I - H - \Sigma_L(E_z) - \Sigma_R(E_z)]^{-1}, \qquad (19)$$

without any self-consistent solution requirements where [H] is Hamiltonian of the isolated system, and $[\Sigma_L]/[\Sigma_R]$ are the self-energies due to the source/drain contacts. Here the matrices have twice the size of the channel region in the corresponding presentation due to the electron spin states. Accordingly, in real space representation for a discrete lattice whose points are located at $x=ja$, j being an integer $(j=1\cdots N)$, the matrix $[E_zI-H-\Sigma_L(E_z)-\Sigma_R(E_z)]$ can be expressed as

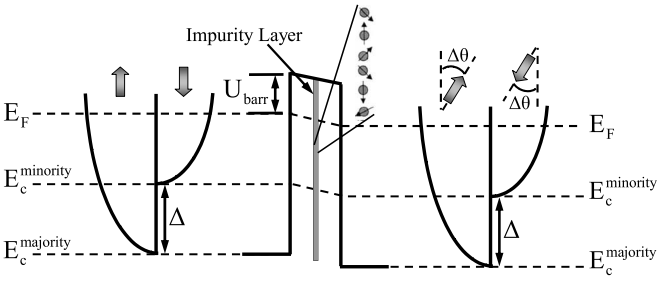

FIG. 2. Energy band diagram for the model MTJs considered here.

$$E_z - H - \Sigma_L - \Sigma_R = \begin{matrix} \\ \langle 1| \\ \langle 2| \\ \\ \langle N-1| \\ \langle N| \end{matrix} \begin{matrix} \begin{matrix} |1\rangle & |2\rangle & & |N-1\rangle & |N\rangle \end{matrix} \\ \begin{bmatrix} E_z I - \alpha_1 - \bar{\Sigma}_L & \beta & \cdots & \bar{0} & \bar{0} \\ \beta^+ & E_z I - \alpha_2 & \cdots & \bar{0} & \bar{0} \\ \vdots & \vdots & \ddots & \vdots & \vdots \\ \bar{0} & \bar{0} & \cdots & E_z I - \alpha_{N-1} & \beta \\ \bar{0} & \bar{0} & \cdots & \beta^+ & E_z I - \alpha_N - \bar{\Sigma}_R \end{bmatrix} \end{matrix}, \tag{20}$$

where α_n is a 2×2 on-site matrix

$$\alpha_n = \begin{bmatrix} E_{c,n}^{\uparrow} + 2t + U_n & 0 \\ 0 & E_{c,n}^{\downarrow} + 2t + U_n \end{bmatrix} \tag{21}$$

and $\beta = -t\bar{I}$ is a 2×2 site-coupling matrix with $\hbar^2/2ma^2$ and $\bar{I} = \left(\begin{smallmatrix} 1 & 0 \\ 0 & 1 \end{smallmatrix}\right)$. The left contact self-energy matrix is nonzero only for the first 2×2 block

$$\Sigma_L(1,1;E_z) = \bar{\Sigma}_L = \begin{bmatrix} -te^{ik_L^{\uparrow}a} & 0 \\ 0 & -te^{ik_L^{\downarrow}a} \end{bmatrix}, \tag{22}$$

where $E_z = E_c^{\uparrow,\downarrow} + U_L + 2t(1-\cos k_L^{\uparrow,\downarrow}a)$. For the right contact only the last block is nonzero:

$$\Sigma_R(N,N,E_z) = \bar{\Sigma}_R = \tilde{\Re} \begin{bmatrix} -te^{ik_R^{\uparrow}a} & 0 \\ 0 & -te^{ik_R^{\downarrow}a} \end{bmatrix} \tilde{\Re}^{\dagger}, \tag{23}$$

where $E_z = E_c^{\uparrow,\downarrow} + U_R + 2t(1-\cos k_R^{\uparrow,\downarrow}a)$ with $\tilde{\Re}$ being the unitary rotation operator defined as

$$\tilde{\Re}(\Delta\theta) = \begin{bmatrix} \cos(\Delta\theta/2) & \sin(\Delta\theta/2) \\ -\sin(\Delta\theta/2) & \cos(\Delta\theta/2) \end{bmatrix}, \tag{24}$$

for two contacts with magnetization directions differing by an angle $\Delta\theta$.

Now the current is calculated using Eqs. (16) with the spectral function obtained from

$$A(E_z) = i[G(E_z) - G^{\dagger}(E_z)], \tag{25}$$

instead of Eq. (8).

A theoretical analysis of MTJ devices in the absence of magnetic impurity layers is presented and compared with the experimental data[5,7] for varying tunneling barrier heights and thicknesses. The parameters used here for the generic ferromagnetic contacts are the Fermi energy $E_F = 2.2$ eV and the exchange field $\Delta = 1.45$ eV.[11] The tunneling region potential barrier $[U_{\text{barr.}}]$ is parametrized within the band gaps quoted from the literature,[12,13] while the charging potential $[U]$ is neglected due to the pure tunneling nature of the transport.

Coherent tunneling regime features are obtained by benchmarking the experimental measurements made in im-

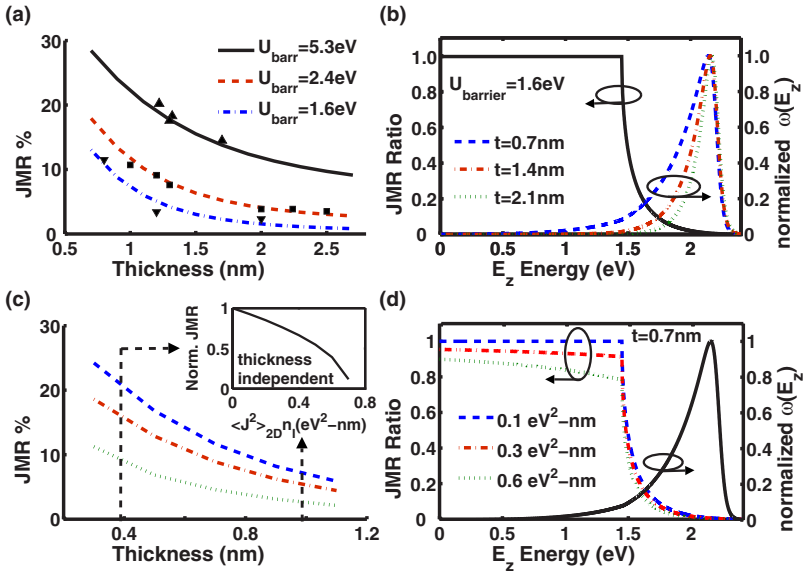

FIG. 3. (Color online) For impurity free MTJs, (a) thickness dependence of JMRs for different barrier heights are shown in comparison with experimental measurements (Refs. 15–24) while an (b) energy resolved analysis of JMR(E_z) (left axis) and normalized $w(E_z)$ (right axis) distributions is also presented for a device with a tunneling barrier height of 1.6 eV. For MTJs with impurity layers, (c) variation of JMRs for varying barrier thicknesses and interactions strengths ($\langle J^2\rangle_{2D} n_I = 0/3/6$ eV^2 nm) are shown together with (d) an energy resolved analysis. Normalized JMRs are proven to be thickness independent as displayed in the inset.

purity free tunneling oxide MTJs at small bias voltages. Referring to I_F/I_{AF} as the current values for the parallel/antiparallel magnetizations ($\Delta\theta=0/\Delta\theta=\pi$) of the ferromagnetic contacts, the JMR is defined as:

$$\mathrm{JMR} = (I_F - I_{AF})/I_F. \tag{26}$$

The dependence of the JMRs on the thickness and the height of the tunneling barriers is shown in Fig. 3(a) with an energy resolved analysis [Fig. 3(b)] for different barrier thicknesses (0.7–1.4–2.1 nm). JMR values are shown to be improving with increasing barrier heights for all barrier thicknesses, a theoretically predicted[7,8,14] and experimentally observed[15–24] feature in MTJs. The barrier heights obtained here may differ from those reported in literature[15–24] based on empirical models.[25]

Experiments and theoretical calculations observe deterioration of JMRs with increasing barrier thicknesses [Fig. 3(a)]. Whereas an energy resolved theoretical analysis shows that energy by energy junction magnetoresistances defined as

$$\mathrm{JMR}(E_z) = [I_F(E_z) - I_{AF}(E_z)]/I_F(E_z), \tag{27}$$

remain unchanged [Fig. 3(b)]. This initially counter intuitive observation can be understood by considering the redistribution of tunneling electron densities over energies with changing tunneling barrier thicknesses. Defining $w(E_z)$ as a measure of the contributing weight of the $\mathrm{JMR}(E_z)$, one can show that experimentally measured JMR is a weighted integral of $\mathrm{JMR}(E_z)$s over E_z energies

$$\mathrm{JMR} = \int \omega(E_z)[\mathrm{JMR}(E_z)]dE_z, \tag{28}$$

where $\omega(E_z)=I_F(E_z)/I_F$ is the energy resolved spin-continuum current component (weighting function). In Eq. (28), independently from the barrier thicknesses $\mathrm{JMR}(E_z)$ ratios are constant [solid line in Fig. 3(b)], while the normalized $\omega(E_z)$ distributions shifts towards higher energies with increasing barrier thicknesses [dashed lines in Fig. 3(b)]. Hence JMRs, an integral of the multiplication of the $\omega(E_z)$ distributions with the energy resolved $\mathrm{JMR}(E_z)$s, decreases with increasing barrier thicknesses [Eq. (26)].

B. Incoherent regime

Spin exchange scattering processes are responsible from the incoherent nature of the tunneling transport for the model devices considered here. Such processes in general may or may not involve energy exchange between the tunneling electrons and the localized spins depending on $\hbar\omega_q$, the energy difference between the spin states. Their incoherent nature arises from our assumption that unspecified external forces continuously restore the localized spins into a state of equilibrium. Their effect on the tunneling electrons cannot be included in the Hamiltonian and are included through an appropriately determined scattering self-energy as described below.

As discussed in Sec. II, coupling between the number of available electrons/holes ($[G^n][G^p]$) at a state and the in/outflow ($[\Sigma_S^{\mathrm{in}}]/[\Sigma_S^{\mathrm{out}}]$) to/from that state is related through the fourth order scattering tensor $[D^n][D^p]$ in Eq. (11). For the model systems considered here, the spin-conserving NSF scattering tensor elements [Eq. (15)] are neglected due to their minor effect on the JMRs and magnetic impurity spin states are assumed degenerate ($\hbar\omega_q=0$) allowing only elastic spin-flip transitions. Accordingly, for large cross-section multilayer devices in a discrete lattice with spacings a,

$$\delta(r-r')\sum_{\omega_q}\langle J^2\rangle N_I(\omega_q) \to \frac{1}{a}\langle J^2\rangle_{2\mathrm{D}} n_I \tag{29}$$

and $[D^n]/[D^p]$ scattering tensors are given by

$$[D^{n,p}]_{\mathrm{SF}} = \langle J^2\rangle_{2\mathrm{D}} n_I/a \begin{array}{c} |\sigma_k\sigma_l\rangle \to \\ \langle\sigma_i\sigma_j|\downarrow \end{array} \begin{array}{c} \\ \langle\uparrow\uparrow| \\ \langle\downarrow\downarrow| \\ \langle\uparrow\downarrow| \\ \langle\downarrow\uparrow| \end{array} \begin{array}{c} \begin{array}{cccc} |\uparrow\uparrow\rangle & |\downarrow\downarrow\rangle & |\uparrow\downarrow\rangle & |\downarrow\uparrow\rangle \end{array} \\ \begin{bmatrix} 0 & F_{u,d} & 0 & 0 \\ F_{u,d} & 0 & 0 & 0 \\ 0 & 0 & 0 & 0 \\ 0 & 0 & 0 & 0 \end{bmatrix} \end{array}, \tag{30}$$

where $n_I=N_I/S$ is the impurity concentration per unit area (S being the device cross section), and $\langle J^2\rangle_{2\mathrm{D}}$ is a parameter reflecting the spin scattering strength of the impurity layer. The $\langle J^2\rangle_{2\mathrm{D}}$ values can be obtained from the available experimental data and are independent from the device cross section S and the lattice grid spacing a used in the calculations. Following this treatment [Eq. (30)], the spin scattering tensor relationship given in Eqs. (11), (14), and (15) will simplify to

$$\Sigma^{\mathrm{in,out}}_{S;\sigma_i\sigma_j}(E) = \sum_{\sigma_k\sigma_l}[D^{n,p}_{\sigma_i\sigma_j;\sigma_k\sigma_l}]_{SF} G^{n,p}_{\sigma_k\sigma_l}(E). \tag{31}$$

A formal derivation of the scattering tensor in Eq. (14) is supplemented in Appendix A. However, the simplified version given in Eq. (30) can be understood heuristically from elementary arguments. For the corresponding lattice site j with magnetic impurities, the in/out-scattering into spin-up component is proportional to the density of the spin-down

electrons/holes times the number of spin-up impurities per unit area $n_I F_u$:

$$(\Sigma^{\text{in,out}}_{S;\uparrow\uparrow})_{j,j} = \frac{1}{a}\langle J^2\rangle_{2D} n_I F_u (G^{n,p}_{\downarrow\downarrow})_{j,j}. \tag{32}$$

Similarly, the in/out-scattering into spin-down component is proportional to the density of the spin-up electrons/holes times the number of spin-down impurities per unit area $n_I F_d$:

$$(\Sigma^{\text{in,out}}_{S;\downarrow\downarrow})_{j,j} = \frac{1}{a}\langle J^2\rangle_{2D} n_I F_d (G^{n,p}_{\uparrow\uparrow})_{j,j}. \tag{33}$$

For pointlike spin exchange scatterings, $[\Sigma^{\text{in}}_S]/[\Sigma^{\text{out}}_S]$ in/out-scattering matrix is block diagonal:

$$\Sigma^{\text{in,out}}_S = \begin{array}{c} \\ \langle 1| \\ \langle 2| \\ \\ \langle N-1| \\ \langle N| \end{array} \begin{array}{c} \begin{array}{cccccc} |1\rangle & |2\rangle & & |N-1\rangle & |N\rangle \end{array} \\ \begin{bmatrix} (\bar{\Sigma}^{\text{in,out}}_S)_{1,1} & \bar{0} & \cdots & \bar{0} & \bar{0} \\ \bar{0} & (\bar{\Sigma}^{\text{in,out}}_S)_{2,2} & \cdots & \bar{0} & \bar{0} \\ \vdots & \vdots & \ddots & \vdots & \vdots \\ \bar{0} & \bar{0} & \cdots & (\bar{\Sigma}^{\text{in,out}}_S)_{N-1,N-1} & \bar{0} \\ \bar{0} & \bar{0} & \cdots & \bar{0} & (\bar{\Sigma}^{\text{in,out}}_S)_{N,N} \end{bmatrix} \end{array}, \tag{34}$$

with the (2×2) block diagonal elements

$$(\bar{\Sigma}^{\text{in,out}}_S)_{j,j} = \begin{array}{c} |\sigma_j\rangle \rightarrow \\ \langle\sigma_i| \downarrow \\ \\ \langle\uparrow| \\ \langle\downarrow| \end{array} \begin{array}{c} \begin{array}{cc} |\uparrow\rangle & |\downarrow\rangle \end{array} \\ \begin{bmatrix} (\Sigma^{\text{in,out}}_{S;\uparrow\uparrow}) & 0 \\ 0 & (\Sigma^{\text{in,out}}_{S;\downarrow\downarrow}) \end{bmatrix}_{j,j} \end{array}. \tag{35}$$

For equally distributed spin-up and spin-down populations of magnetic impurities ($F_u = F_d = 0.5$), $[D^n]_{sf}$ and $[D^p]_{sf}$ scattering tensors are equal,

$$[D^n]_{SF} = [D^p]_{SF} = D. \tag{36}$$

Under these conditions, using Eqs. (3), (5), and (31), and through the definition of spectral energy $A(E)$ [Eq. (8)], it can be shown that there is a simple relationship between the device Green's function and the spin scattering self-energy,

$$\Sigma_{S;\sigma_i\sigma_j}(E) = \sum_{\sigma_k\sigma_l} [D_{\sigma_i\sigma_j;\sigma_k\sigma_l}] G_{\sigma_k\sigma_l}(E). \tag{37}$$

This assumption ($D^n = D^p$) simplifies the treatment of scattering processes significantly for two distinct reasons. First, Eq. (37) allows us to obtain $[\Sigma_S]$ without using the Hilbert transformations [Eq. (4)]. More importantly, it decouples the solution of $[G]/[\Sigma_S]$ from the solution of $[G^n]/[\Sigma^{\text{in}}_S]$ making it possible to use $f_{2D}(E_z - \mu_{L,R})$ functions [see Eq. (17)] to represent the sum over the transverse momentum as in the coherent regime. The overall procedure can now be summarized in two steps.

(i) Greens' function $[G]$ and scattering self-energy $[\Sigma_S]$ matrices are calculated in a self-consistent manner using Eqs. (6), (7), and (37) with

$$G(E_z) = [E_z I - H - U - \Sigma_L(E_z) - \Sigma_R(E_z) - \Sigma_S(E_z)]^{-1} \tag{38a}$$

$$\Sigma_S(E_z, \varepsilon_{\vec{k}_\parallel}) = \Sigma_S(E_z), \tag{38b}$$

where due to the decoupling of the 2D translational modes, operators are independent from the transverse energy $\varepsilon_k = \hbar^2 k^2/2m$ of the tunneling electrons [see also Eqs. (22) and (23)].

(ii) Electron correlation function $[G^n]$ and in-scattering matrix $[\Sigma^{\text{in}}_S]$ can be obtained noniteratively from Eqs. (11) and (31) and using the Greens function $G(E_z)$ obtained in the previous self-consistent loop (as shown in Appendix B):

$${}^{2D}\Sigma^{\text{in}}_{S,\sigma_i\sigma_j}(E_z) = \sum_{\sigma_k,\sigma_l} [D_{\sigma_i\sigma_j;\sigma_k\sigma_l}]\, {}^{2D}G^n_{\sigma_k\sigma_l}(E_z), \tag{39}$$

where the 2D integrated versions of the inscattering and correlation functions are defined as

$${}^{2D}G^n(E_z) = \sum_{\varepsilon_{\vec{k}_\parallel}} G^n(E_z, \varepsilon_{\vec{k}_\parallel}), \tag{40a}$$

$${}^{2D}\Sigma^{\text{in}}_S(E_z) = \sum_{\varepsilon_{\vec{k}_\parallel}} \Sigma^{\text{in}}_S(E_z, \varepsilon_{\vec{k}_\parallel}). \tag{40b}$$

One important point to note here is that for elastic spin scattering processes there is no need to calculate 2D integrated $[G^p]$ hole correlation function and $[\Sigma^{\text{out}}_S]$ outscattering matrix. Spectral function $[A(E_z)]$ used in the current relation (16b) can be directly obtained from Eq. (8) using the device Green's function $G(E_z)$ obtained in the previous self-consistent loop.

The incoherent tunneling regime device characteristics in the presence of magnetic impurities is studied for a fixed barrier height $U_{\text{barr}} = 1.6$ eV [Fig. 3(c)] with changing barrier thicknesses ($t = 0.3 - 1.1$ nm) and electron-impurity spin exchange interactions ($\langle J^2\rangle_{2D} n_I = 0/3/6$ eV^2 nm). Nonlinear decreasing JMRs with increasing spin-exchange interactions

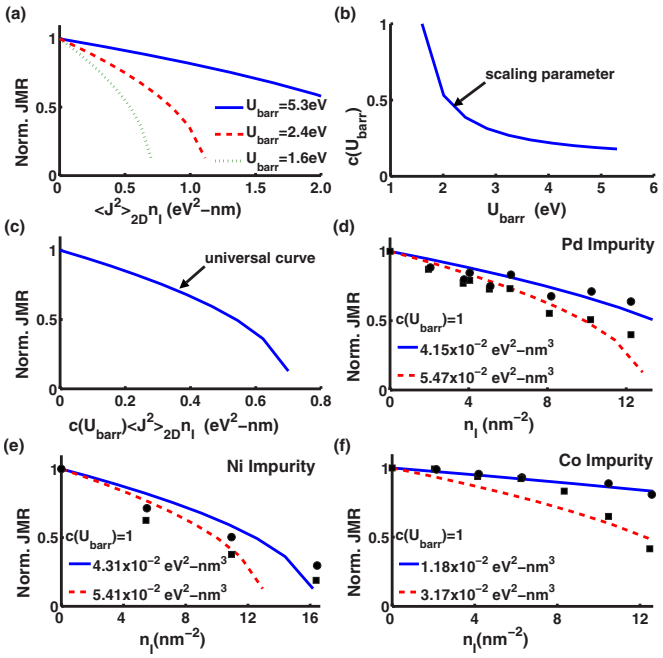

FIG. 4. (Color online) (a) Normalized JMRs deteriorates with increasing spin-dephasing strenghts independently from the tunneling barrier heights. (b) Using a barrier height dependent scaling parameter $c(U_{\mathrm{barr}})$, (c) this general trend can be scaled to a single universal curve. Experimental data taken at 77 K (solid) and 300 K (dashed) is compared with theoretical analysis in the presence of (d) Pd, (e) Ni and (f) Co magnetic impurities with increasing impurity concentrations for a scaling constant $c(U_{\mathrm{barr}})=1$.

are observed at all barrier thicknesses due to the mixing of independent spin-channels[5,6] while the normalized JMRs are proven to be thickness independent (inset). This observation is attributed to the elastic nature of the spin exchange interactions yielding a total drop in JMR(E_z) values at all E_z energies in Eq. (26) while preserving the normalized $\omega(E_z)$ carrier distributions [Fig. 3(d)].

Further analysis shows that normalized JMRs deteriorate with increasing spin-dephasing strengths ($\langle J^2\rangle_{2\mathrm{D}} n_I$) independently from the tunneling barrier heights [Figs. 4(a)–4(c)]. This general trend can be shown by mapping the normalized JMRs into a single universal curve using a tunneling barrier height dependent scaling constant $c(U_{\mathrm{barr}})$ [Fig. 4(b)].

This allows us to choose a particular value of barrier height [$U_{\mathrm{barr}}=1.6$ eV] and adjust a single parameter $\langle J^2\rangle_{2\mathrm{D}}$ tofit our NEGF calculations [Figs. 4(d)–4(f)] with experimental measurements obtained from δ-doped MTJs.[5] Here the submonolayer impurity thicknesses (t) given in the measurements are converted into impurity concentrations per area (n_I) using $n_I=t\times n_{\mathrm{bulk}}$ where n_{bulk} is the bulk material density of the Pd/Ni/Co impurities.[5]

Close fitting to the experimental data are observed at 77 K [Figs. 4(d)–4(f)] (solid line) for devices with Pd/Ni/Co impurities.[26] However, the experimentally observed temperature dependence of normalized JMR ratios cannot be accounted for by our model calculations. Broadenings of the electrodes' Fermi distributions due to changing temperatures from 77 to 300 K seem to yield variations in normalized JMR ratios within a linewidth. As a result, different $\langle J^2\rangle_{2\mathrm{D}}$ couplings are used in order to match the experimental data taken at 300 K.

For Pd and Ni doped MTJs, relatively small variations in exchange coupling parameters are needed $\langle J^2_{300\ \mathrm{K}}\rangle_{2\mathrm{D}}/\langle J^2_{77\ \mathrm{K}}\rangle_{2\mathrm{D}}=1.32$ (for Pd) and $\langle J^2_{300\ \mathrm{K}}\rangle_{2\mathrm{D}}/\langle J^2_{77\ K}\rangle_{2\mathrm{D}}=1.25$ (for Ni) in order to match the experimental data at 300 K (dashed line). These small temperature dependences could be due to the presence of some secondary mechanisms not included in our calculations. One such mechanism reported in literature is the impurity-assisted conductance contribution through the defects (possibly created by the inclusion of magnetic impurities within the barrier) which is known to be strongly temperature dependent.[27] In fact, the contribution of the impurity-assistant conductance is proportional with the impurity concentrations in accordance with the experimental measurements.

Another interesting feature observed in calculations [Figs. 4(d) and 4(e)] is the comparable $\langle J^2\rangle_{2\mathrm{D}}$ couplings for the Pd and Ni impurities at temperatures 77 and 300 K. Accordingly, a possible estimate of the impurity spin states may be made by considering the most commonly encountered oxidation states of the Pd and Ni impurities. Closed-shell elemental Pd is only known to be in a magnetic oxidized state of $S=1$ in octahedral oxygen coordination according to the Hund's rules.[28] Similarly, we may attribute the comparable $\langle J^2\rangle_{2\mathrm{D}}$ couplings for Ni impurities due to the $S=1$ spin state of the Ni^{+2} which is known to be a frequently observed ionized state in oxygen environment.[29]

On the contrary, for Co doped MTJs, there is a clear distinction for normalized JMR ratios at different temperatures [Fig. 4(f)] which cannot be justified by the presence of secondary mechanisms. Fitting these large deviations require large variations in $\langle J^2\rangle_{2\mathrm{D}}$ exchange coupling parameters [$(\langle J^2_{300\ \mathrm{K}}\rangle_{2\mathrm{D}}/\langle J^2_{77\ \mathrm{K}}\rangle_{2\mathrm{D}}=2.69)$]. We propose this to be a result of thermally driven low-spin/high-spin phase transition.[30,31] This is a credible argument since the oxidation state of the cobalt atoms can be in Co^{+2} ($S=3/2$, high-spin) or Co^{+3} ($S=0$, low-spin) state or partially in both of the states depending on the oxidation environment. Such thermally driven low-spin/high-spin phase transitions for metal oxides have been predicted by theoretical calculations and observed in experimental studies.[30,31] These phase transitions have not been discussed in MTJs community in connection with possible scattering factors determining the temperature dependence of JMRs. Although from the available experimental data it is not possible to make a decisive conclusion in this direction, given the nonlinear dependence of JMRs on magnetic impurity states in our calculations, we believe that it's important to point out this possibility here.

An order of magnitude analysis of $\langle J^2\rangle_{2D}$ exchange interaction parameters obtained in this article can be done using $\langle J^2\rangle=a_0{}^3\langle J^2\rangle_{2\mathrm{D}}$, where $a_0{}^3$ is a normalization volume related to the wave function overlapping. For our purposes, it is enough to assume a_0 equal to the Bohr radius. Accordingly, $\sqrt{\langle J^2\rangle}$ values are within a physically reasonable range of 1.3–2.9 meV nm^3 in accordance with the *ab initio* calculations.[32]

IV. SUMMARY

A NEGF-based quantum transport model incorporating spin-flip scattering processes within the self-consistent Born approximation is presented. Spin-flip scattering and quantum effects are simultaneously captured. Spin scattering operators are derived for the specific case of electron-impurity spin-exchange interactions and the formalism is applied to spin-dependent electron transport in MTJs with magnetic impurity layers. The theory is benchmarked against experimental data involving both coherent and incoherent transport regimes. JMRs are shown to decrease both with barrier thickness and spin-flip scattering but our unified treatment clearly brings out the difference in the underlying physics (Fig. 3). Our numerical results show that both barrier height and the exchange interaction constant $\langle J^2\rangle_{2D}$ can be subsumed into a single parameter that can explain a variety of experiments [Fig. 4(d) and 4(e)]. Small differences in spin-states and concentrations of magnetic impurities are shown to cause large deviations in JMRs. Interesting similarities and differences among devices with Pd, Ni and Co impurities are pointed out, which could be signatures of the spin states of oxidized Pd and Ni impurities and low-spin/high-spin phase transitions for oxidized Co impurities.

ACKNOWLEDGMENTS

This work was supported by the MARCO focus center for Materials, Structure and Devices and the NSF Network for Computational Nanotechnology. nanoHUB.org computational resources were used. Part of this work was carried out at the Jet Propulsion Laboratory under a contract with the National Aeronautics and Space Administration NASA funded by ARDA and ARO.

APPENDIX A: SPIN EXCHANGE SCATTERING TENSOR

In the following, the scattering tensors stated in Eqs. (14) and (15) of the main paper are obtained starting from standard expressions obtained in the self-consistent Born approximation from the NEGF formalism. Here we start from the formulation in Ref. 9 (see Secs. 10.4 and A.4) which represents a generalization of the earlier treatments[33–36] (also check Ref. 37). For spatially localized scatterers we have

$$D^n_{\sigma_i\sigma_j;\sigma_k\sigma_l}(\xi;\xi') = \left\langle \sum_{s_\beta,s_\alpha} \tau_{\sigma_i s_\alpha;\sigma_k s_\beta}(\xi)\tau^*_{\sigma_j s_\alpha;\sigma_l s_\beta}(\xi') \right\rangle = \left\langle \sum_{s_\alpha,s_\beta} \langle s_\alpha|H_{I;\sigma_i\sigma_k}(\xi)|s_\beta\rangle\langle s_\beta|H^\dagger_{I;\sigma_l\sigma_j}(\xi')|s_\alpha\rangle \right\rangle, \tag{A1a}$$

$$D^p_{\sigma_i\sigma_j;\sigma_k\sigma_l}(\xi;\xi') = \left\langle \sum_{s_\beta,s_\alpha} \tau_{\sigma_l s_\beta;\sigma_j s_\alpha}(\xi)\tau^*_{\sigma_k s_\beta;\sigma_i s_\alpha}(\xi') \right\rangle = \left\langle \sum_{s_\alpha,s_\beta} \langle s_\beta|H_{I;\sigma_i\sigma_j}(\xi)|s_\alpha\rangle\langle s_\alpha|H^\dagger_{I;\sigma_i\sigma_k}(\xi')|s_\beta\rangle \right\rangle, \tag{A1b}$$

where $|s_\alpha\rangle$ and $|s_\beta\rangle$ are impurity spin subspace states and H_I is the interaction Hamiltonian [Eq. (12)] defined within the channel electron spin subspace as

$$H_{I;\sigma_i\sigma_k/\sigma_l\sigma_j}(\xi) = \langle\sigma_i/\sigma_l|H_I(r,t)|\sigma_k/\sigma_j\rangle, \tag{A2a}$$

$$H^\dagger_{I;\sigma_i\sigma_k/\sigma_l\sigma_j}(\xi') = \langle\sigma_i/\sigma_l|H^\dagger_I(r',t')|\sigma_k/\sigma_j\rangle. \tag{A2b}$$

For an uncorrelated impurity spin ensemble with

$$\rho = \sum_{s_\alpha} w_{s_\alpha}|s_\alpha\rangle\langle s_\alpha| = \sum_{s_\beta} w_{s_\beta}|s_\beta\rangle\langle s_\beta| \tag{A3}$$

averaging in Eqs. (A1a) and (A1b) can be done through a weighted summation of spin scattering rates of magnetic impurities:

$$\begin{aligned} D^n_{\sigma_i\sigma_j;\sigma_k\sigma_l}(r,t;r',t') &= \sum_{s_\alpha,s_\beta} w_{s_\beta}\langle s_\alpha|H_{I;\sigma_i\sigma_k}(r,t)|s_\beta\rangle\langle s_\beta|H^\dagger_{I;\sigma_l\sigma_j}(r',t')|s_\alpha\rangle = \sum_{s_\alpha}\langle s_\alpha|H_{I;\sigma_i\sigma_k}(r,t)[\rho]H^\dagger_{I;\sigma_l\sigma_j}(r',t')|s_\alpha\rangle \\ &= \mathrm{tr}[\rho H^\dagger_{I;\sigma_l\sigma_j}(r',t')H_{I;\sigma_i\sigma_k}(r,t)], \end{aligned} \tag{A4a}$$

$$\begin{aligned} D^p_{\sigma_i\sigma_j;\sigma_k\sigma_l}(r,t;r',t') &= \sum_{s_\alpha,s_\beta} w_{s_\alpha}\langle s_\beta|H_{I;\sigma_l\sigma_j}(r,t)|s_\alpha\rangle\langle s_\alpha|H^\dagger_{I;\sigma_i\sigma_k}(r',t')|s_\beta\rangle = \sum_{s_\beta}\langle s_\beta|H_{I;\sigma_l\sigma_j}(r,t)[\rho]H^\dagger_{I;\sigma_i\sigma_k}(r',t')|s_\beta\rangle \\ &= \mathrm{tr}[\rho H^\dagger_{I;\sigma_i\sigma_k}(r',t')H_{I;\sigma_l\sigma_j}(r,t)]. \end{aligned} \tag{A4b}$$

The trace $\mathrm{tr}(\rho A)$ for any operator A is independent of representation. Accordingly, $[D^n]/[D^p]$ scattering tensors can be evaluated using any convenient basis for magnetic impurity spin states.

Through Jordan-Wigner transformation, single spins can be thought as an empty or singly occupied fermion state

$$|\uparrow\rangle \equiv a^+|0\rangle, \tag{A5a}$$

$$|\downarrow\rangle \equiv |0\rangle, \tag{A5b}$$

with creation/annihilation operators for the channel electrons

$$a^+(t) = \sigma^+(t) = \begin{bmatrix} 0 & e^{i\omega_e t} \\ 0 & 0 \end{bmatrix}, \tag{A6a}$$

$$a(t) = \sigma^-(t) = \begin{bmatrix} 0 & 0 \\ e^{-i\omega_e t} & 0 \end{bmatrix}. \tag{A6b}$$

For degenerate electron spin states ($\hbar\omega_e = 0$), there is no time dependence as such $a^\dagger(t) \to a^\dagger$, $a(t) \to a$.

Pauli spin matrices are related to creation/annihilation operators through $\sigma_x = (a^\dagger + a)/2$, $\sigma_y = (a^\dagger + a)/2i$ and $\sigma_z = a^\dagger a - 1/2$. Accordingly, interaction Hamiltonian $H_I(r,t) = J\delta(\vec{r} - \vec{R})\vec{\sigma}\cdot\vec{S}(t)$ can be expressed as

$$H_I(r,t) = J\delta(\vec{r} - \vec{R})\left[\frac{1}{2}aS_+(t) + \frac{1}{2}a^\dagger S_-(t) + \left(a^\dagger a - \frac{1}{2}\right)S_Z(t)\right], \tag{A7}$$

where S is the spin operator for the localized magnetic impurity.

Substituting the interaction Hamiltonian from Eq. (A7) into Eqs. (A4a) and (A4b) will yield

$$H^\dagger_{I;\sigma_l\sigma_j}(r',t')H_{I;\sigma_i\sigma_k}(r,t) = \delta(r-r') \begin{array}{c} |\sigma_k\sigma_l\rangle \to \\ \langle\sigma_i\sigma_j| \downarrow \end{array} \begin{array}{c} \\ \langle\uparrow\uparrow| \\ \langle\downarrow\downarrow| \\ \langle\uparrow\downarrow| \\ \langle\downarrow\uparrow| \end{array} \begin{array}{c} \begin{array}{cccc} |\uparrow\uparrow\rangle & |\downarrow\downarrow\rangle & |\uparrow\downarrow\rangle & |\downarrow\uparrow\rangle \end{array} \\ \begin{bmatrix} S_Z(t')S_Z(t) & S_+(t')S_-(t) & S_+(t')S_Z(t) & S_Z(t')S_-(t) \\ S_-(t')S_+(t) & S_Z(t')S_Z(t) & -S_Z(t')S_+(t) & -S_-(t')S_Z(t) \\ S_-(t')S_Z(t) & -S_Z(t')S_-(t) & -S_Z(t')S_Z(t) & S_-(t')S_-(t) \\ S_Z(t')S_+(t) & -S_+(t')S_Z(t) & S_+(t')S_+(t) & -S_Z(t')S_Z(t) \end{bmatrix} \end{array}, \tag{A8a}$$

$$H^\dagger_{I;\sigma_i\sigma_j}(r',t')H_{I;\sigma_l\sigma_j}(r,t) = \delta(r-r') \begin{array}{c} |\sigma_k\sigma_l\rangle \to \\ \langle\sigma_i\sigma_j| \downarrow \end{array} \begin{array}{c} \\ \langle\uparrow\uparrow| \\ \langle\downarrow\downarrow| \\ \langle\uparrow\downarrow| \\ \langle\downarrow\uparrow| \end{array} \begin{array}{c} \begin{array}{cccc} |\uparrow\uparrow\rangle & |\downarrow\downarrow\rangle & |\uparrow\downarrow\rangle & |\downarrow\uparrow\rangle \end{array} \\ \begin{bmatrix} S_Z(t')S_Z(t) & S_-(t')S_+(t) & S_Z(t')S_+(t) & S_-(t')S_Z(t) \\ S_+(t')S_-(t) & S_Z(t')S_Z(t) & -S_+(t')S_Z(t) & -S_Z(t')S_-(t) \\ S_Z(t')S_-(t) & -S_-(t')S_Z(t) & -S_Z(t')S_Z(t) & S_-(t')S_-(t) \\ S_+(t')S_Z(t) & -S_Z(t')S_+(t) & S_+(t')S_+(t) & -S_Z(t')S_Z(t) \end{bmatrix} \end{array}. \tag{A8b}$$

The localized magnetic impurity spin-operators can be written in its diagonalized impurity spin subspace as

$$S_+ = d^\dagger = \begin{bmatrix} 0 & e^{i\omega_q t} \\ 0 & 0 \end{bmatrix}, \tag{A9a}$$

$$S_- = d = \begin{bmatrix} 0 & 0 \\ e^{-i\omega_q t} & 0 \end{bmatrix}, \tag{A9b}$$

$$S_Z = d^\dagger d - \frac{1}{2} = \frac{1}{2}\begin{bmatrix} 1 & 0 \\ 0 & -1 \end{bmatrix} \tag{A9c}$$

with $\omega_q = \Delta E_I/\hbar$ where ΔE_I is the energy difference between spin-up and spin-down states for the localized magnetic impurities.

For a given impurity density matrix of the form $(F_u + F_d = 1)$:

$$\rho = N_I(\omega_q)\begin{bmatrix} F_u & 0 \\ 0 & F_d \end{bmatrix}, \tag{A10}$$

with N_I being total number of impurities at that location, the desired quantities $[D^n]/[D^p]$ can be obtained by evaluating the expectation values of the operators in Eqs. (A8a) and (A8b). Here the only nonzero elements are

$$\mathrm{tr}[\rho S_Z(t')S_Z(t)] = \frac{1}{4}, \tag{A11a}$$

$$\mathrm{tr}[\rho S_+(t')S_-(t)] = F_u e^{-i\omega_q(t-t')}, \tag{A11b}$$

$$\mathrm{tr}[\rho S_-(t')S_+(t)] = F_d e^{i\omega_q(t-t')}. \tag{A11c}$$

Finally, for a given impurity density matrix [Eq. (A10)], $[D^n]/[D^p]$ tensors are obtained as

$$D^n(r,t;r',t') = \delta(r-r')\sum_{\omega_q}\langle J^2\rangle N_l(\omega_q)\begin{matrix}\langle\uparrow\uparrow|\\ \langle\downarrow\downarrow|\\ \langle\uparrow\downarrow|\\ \langle\downarrow\uparrow|\end{matrix}\begin{matrix}\begin{matrix}|\uparrow\uparrow\rangle & |\downarrow\downarrow\rangle & |\uparrow\downarrow\rangle & |\downarrow\uparrow\rangle\end{matrix}\\ \begin{bmatrix}1/4 & F_u e^{-i\omega_q(t-t')} & 0 & 0\\ F_d e^{i\omega_q(t-t')} & 1/4 & 0 & 0\\ 0 & 0 & -1/4 & 0\\ 0 & 0 & 0 & -1/4\end{bmatrix}\end{matrix}, \quad \begin{matrix}|\sigma_k\sigma_l\rangle\rightarrow\\ \langle\sigma_i\sigma_j|\downarrow\end{matrix} \tag{A12a}$$

$$D^p(r,t;r',t') = \delta(r-r')\sum_{\omega_q}\langle J^2\rangle N_l(\omega_q)\begin{matrix}\langle\uparrow\uparrow|\\ \langle\downarrow\downarrow|\\ \langle\uparrow\downarrow|\\ \langle\downarrow\uparrow|\end{matrix}\begin{matrix}\begin{matrix}|\uparrow\uparrow\rangle & |\downarrow\downarrow\rangle & |\uparrow\downarrow\rangle & |\downarrow\uparrow\rangle\end{matrix}\\ \begin{bmatrix}1/4 & F_d e^{i\omega_q(t-t')} & 0 & 0\\ F_u e^{-i\omega_q(t-t')} & 1/4 & 0 & 0\\ 0 & 0 & -1/4 & 0\\ 0 & 0 & 0 & -1/4\end{bmatrix}\end{matrix}. \quad \begin{matrix}|\sigma_k\sigma_l\rangle\rightarrow\\ \langle\sigma_i\sigma_j|\downarrow\end{matrix} \tag{A12b}$$

It is convenient to work with the Fourier transformed functions as such $(t-t')\rightarrow\hbar\omega$:

$$e^{-i\omega_q(t-t')}e^{-\eta|t-t'|/\hbar} \rightarrow \delta(\hbar\omega-\hbar\omega_q), \tag{A13}$$

where η is a positive infinitesimal. With Fourier transforming Eqs. (A12a) and (A12b) will simplify to Eqs. (14) and (15).[36] For the calculations reported in this article, diagonal elements not leading to spin-dephasing are omitted due to their negligible effect on JMR ratios. In this case $[D^n]/[D^p]$ scattering tensors simplifies to a form [Eq. (30)] which can be understood from simple common-sense arguments [Eqs. (32) and (33)].

APPENDIX B: IN-SCATTERING MATRIX AND CORRELATION FUNCTION

In the following a noniterative solution scheme for $[\Sigma^{\text{in}}]$ in-scattering matrix and $[G^n]$ electron correlation function in the presence of a elastic spin scatterings $(\hbar\omega_q=0)$ is summarized. It is shown that for decoupled transverse modes, 2D integrated $[^{2D}\Sigma_S^{\text{in}}]$ in-scattering matrix and $[^{2D}G^n]$ electron correlation function can be obtained from $f_{2D}(E_z-\mu_{L,R})$ contact Fermi functions [Eq. (17)] through a tensor to matrix transformation.

We start our derivation by redefining Eq. (31) in an energy grid defined in longitudinal (E_z) and transverse $(\varepsilon_{\vec{k}_\parallel})$ directions:

$$\Sigma^{\text{in}}_{S,\sigma_k\sigma_l}(E_z,\varepsilon_{\vec{k}_\parallel}) = \sum_{\sigma_m,\sigma_n}[D_{\sigma_k\sigma_l;\sigma_m\sigma_n}]G^n_{\sigma_m\sigma_n}(E_z,\varepsilon_{\vec{k}_\parallel}), \tag{B1}$$

and using Eqs. (9) and (10), we obtain

$$G^n_{\sigma_i\sigma_j}(E_z,\varepsilon_{\vec{k}_\parallel}) = S^n_{\sigma_i\sigma_j}(E_z,\varepsilon_{\vec{k}_\parallel}) + \sum_{\sigma_m,\sigma_n}[P_{\sigma_i\sigma_j;\sigma_m\sigma_n}(E_z)]G^n_{\sigma_m\sigma_n}(E_z,\varepsilon_{\vec{k}_\parallel}), \tag{B2}$$

where $S^n_{\sigma_i\sigma_j}(E_z,\varepsilon_{\vec{k}_\parallel})$ and $P_{\sigma_i\sigma_j;\sigma_m\sigma_n}(E_z)$ are defined as

$$S^n_{\sigma_i\sigma_j}(E_z,\varepsilon_{\vec{k}_\parallel}) = \sum_{\sigma_k,\sigma_l} G_{\sigma_i\sigma_k}(E_z)[\Sigma^{\text{in}}_{L,\sigma_k\sigma_l}(E_z,\varepsilon_{\vec{k}_\parallel}) + \Sigma^{\text{in}}_{R,\sigma_k\sigma_l}(E_z,\varepsilon_{\vec{k}_\parallel})]G_{\sigma_l\sigma_j}(E_z)^+, \tag{B3a}$$

$$P_{\sigma_i\sigma_j;\sigma_m\sigma_n}(E_z) = \sum_{\sigma_k,\sigma_l} G_{\sigma_i\sigma_k}(E_z)[D_{\sigma_k\sigma_l;\sigma_m\sigma_n}]G^+_{\sigma_l\sigma_j}(E_z). \tag{B3b}$$

Equation (B2) can be integrated over transverse modes using 2D integrated Fermi functions [see Eqs. (17) and (18)] and replacing $\Sigma^{\text{in}}_{L,R;\sigma_i\sigma_j}(E_z,\varepsilon_{\vec{k}_\parallel})$ with $^{2D}\Sigma^{\text{in}}_{L,R;\sigma_i\sigma_j}(E_z)$:

$$\sum_{\varepsilon_{\vec{k}_\parallel}}\left[G^n_{\sigma_i\sigma_j}(E_z,\varepsilon_{\vec{k}_\parallel}) - \sum_{\sigma_m,\sigma_n}[P_{\sigma_i\sigma_j;\sigma_m\sigma_n}(E_z)]G^n_{\sigma_m\sigma_n}(E_z,\varepsilon_{\vec{k}_\parallel})\right] = {}^{2D}S^n_{\sigma_i\sigma_j}(E_z). \tag{B4}$$

Here $^{2D}S^n_{\sigma_i\sigma_j}(E_z)$ refers the 2D integrated sum of the matrix defined in Eq. (B3a). An index transformation as such $\sigma_i\sigma_j\rightarrow J$ and $\sigma_m\sigma_n\rightarrow M$ will convert this tensor relationship into

$$\sum_{\varepsilon_{\vec{k}_\parallel}}\left[\tilde{G}^n_J(E_z,\varepsilon_{\vec{k}_\parallel}) - \sum_M[\tilde{P}_{JM}(E_z)]\tilde{G}^n_M(E_z,\varepsilon_{\vec{k}_\parallel})\right] = {}^{2D}\tilde{S}^n_J(E_z). \tag{B5}$$

This is simply a matrix multiplication in the transformed basis

$$\sum_{\varepsilon_{\vec{k}_\parallel}} \tilde{G}^n(E_z, \varepsilon_{\vec{k}_\parallel}) = (I - \tilde{P}(E_z))^{-1}[{}^{2D}\tilde{S}^n(E_z)], \tag{B6}$$

yielding a only longitudinal energy dependent relation when summed over 2D translational energies

$${}^{2D}\tilde{G}^n(E_z) = \sum_{\varepsilon_{\vec{k}_\parallel}} \tilde{G}^n(E_z, \varepsilon_{\vec{k}_\parallel}). \tag{B7}$$

Electron correlation functions defined in this new basis set can be transformed back to the real space matrix after reindexing with $J \rightarrow \sigma_i \sigma_j$ and $M \rightarrow \sigma_m \sigma_n$:

$${}^{2D}\tilde{G}^n(E_z) \rightarrow {}^{2D}G^n(E_z). \tag{B8}$$

Accordingly, 2D in-scattering function $[{}^{2D}\Sigma_S^{in}]$ can be obtained using Eqs. (31) and (B8) leading to Eq. (39).

*yanik@purdue.edu

[1] R. Landauer, Phys. Scr. **T42**, 110 (1992).
[2] Y. Li and C. R. Chang, Phys. Lett. A **287**, 415 (2001).
[3] Y. Li, C. R. Chang, and Y. D. Yao, J. Appl. Phys. **91**, 8807 (2002).
[4] L. Sheng, D. Y. Xing, and D. N. Sheng, Phys. Rev. B **69**, 132414 (2004).
[5] R. Jansen and J. S. Moodera, J. Appl. Phys. **83**, 6682 (1998).
[6] R. Jansen and J. S. Moodera, Phys. Rev. B **61**, 9047 (1998).
[7] A. H. Davis, Ph. D. thesis, Tulane University, New Orleans, 1994.
[8] A. H. Davis and J. M. Maclaren, J. Phys.: Condens. Matter **14**, 4365 (2002).
[9] S. Datta, *Quantum Transport: Atom to Transistor* (Cambridge University Press, Cambridge, 2005).
[10] J. Appelbaum, Phys. Rev. **154**, 633 (1967).
[11] M. B. Stearns, J. Magn. Magn. Mater. **5**, 167 (1977).
[12] J. S. Moodera, L. R. Kinder, T. M. Wong, and R. Meservey, Phys. Rev. Lett. **74**, 3273 (1995).
[13] V. E. Henrich and P. A. Cox, *The Surface Science of Metal Oxides* (Cambridge University Press, Cambridge, 1994).
[14] J. Mathon, Phys. Rev. B **56**, 11810 (1997).
[15] K. Matsuda, A. Kamijo, T. Mitsuzuka, and H. Tsuge, J. Appl. Phys. **85**, 5261 (1999).
[16] H. Chen, Q. Y. Xu, G. Ni, J. Lu, H. Sang, S. Y. Zhang, and Y. W. Du, J. Appl. Phys. **85**, 5798 (1999).
[17] J. Zhang and R. M. White, J. Appl. Phys. **83**, 6512 (1998).
[18] T. Mitsuzuka, K. Matsuda, A. Kamijo, and H. Tsuge, J. Appl. Phys. **85**, 5807 (1998).
[19] W. Oepts, H. J. Verhagen, R. Coehoorn, and W. J. M. de Jonge, J. Appl. Phys. **86**, 3863 (1999).
[20] R. S. Beech, J. Anderson, J. Daughton, B. A. Everitt, and D. Wang, IEEE Trans. Magn. **32**, 4713 (1996).
[21] H. Yamanaka, K. Saito, K. Takanashi, and H. Fujimori, IEEE Trans. Magn. **35**, 2883 (1999).
[22] J. S. Moodera, J. Nowak, and R. J. M. van de Veerdonk, Phys. Rev. Lett. **80**, 2941 (1998).
[23] J. J. Sun and P. P. Freitas, J. Appl. Phys. **85**, 5264 (1999).
[24] C. H. Shang, J. Nowak, R. Jansen, and J. S. Moodera, Phys. Rev. B **58**, R2917 (1998).
[25] J. G. Simmons, J. Appl. Phys. **34**, 1793 (1963).
[26] B. E. Kane, Nature (London) **393**, 133 (1998).
[27] R. C. S. *et al.*, J. Appl. Phys. **85**, 5258 (1999).
[28] P. A. Cox, *Transition Metal Oxides. An Introduction to their Electronic Structure and Properties* (Clarendon, Oxford, 1992).
[29] S. Geschwind and J. P. Remeika, J. Appl. Phys. **33**, 370 (1962).
[30] T. Kambara, J. Chem. Phys. **70**, 4199 (1979).
[31] S. W. Biernacki and B. Clerjaud, Phys. Rev. B **72**, 024406 (2005).
[32] M. van Schilfgaarde and V. P. Antropov, J. Appl. Phys. **85**, 4827 (1999).
[33] R. Lake, G. Klimeck, R. C. Bowen, and D. Jovanovic, J. Appl. Phys. **81**, 7845 (1997).
[34] S. Datta, J. Phys.: Condens. Matter **2**, 8023 (1990).
[35] G. D. Mahan, Phys. Rep. **145**, 251 (1987).
[36] S. Datta (unpublished).
[37] A heuristic derivation of the $[D^n]/[D^p]$ scattering tensors in the elastic limit was described in Ref. 36. A typo in Eq. (9b) has been corrected here.